Chemical Engineering Research and Design 157 (2020) 34–45

Contents lists available at ScienceDirect

Chemical Engineering Research and Design

journal homepage: www.elsevier.com/locate/cherd

Non-Newtonian fluid flow from bottom of tank using orifices of different shapes

Morakane Khahledi[a,*], *Rainer Haldenwang*[a], *Raj Chhabra*[a,b], *Veruscha Fester*[a]

[a] *Dept. Civil Engineering and Surveying, Cape Peninsula University of Technology, Cape Town, South Africa*
[b] *Dept. Chemical Engineering, IIT Ropar, Rupnagar, 140001, India*

ARTICLE INFO

Article history:
Received 13 December 2019
Received in revised form 11 February 2020
Accepted 16 February 2020
Available online 22 February 2020

Keywords:
Orifices
Discharge coefficient
Reynolds number
Rheology
Viscosity
Tank

ABSTRACT

The use of orifices in measuring and regulating the discharge of Newtonian liquids from tanks has been studied extensively. For non-Newtonian liquids, this is not the case mainly due to the complex rheological properties of such liquids. To date only circular orifices have been used to measure the flow of Power-Law liquids from a tank. In this work, a range of non-Newtonian liquids flowing from a tank through different sizes of sharp crested circular, square and triangular orifices have been tested. A rectangular tank suspended from a weighbridge with a load cell was used and the orifices were fitted at the bottom of the tank for the discharge measurement. The rheological parameters of the test liquids were obtained using a concentric cylinder viscometer. The liquids tested included Newtonian, Power-law, Bingham and Herschel–Bulkley model liquids. The height-time data was transformed into discharge coefficient (C_d)-Reynolds number (Re) format for each liquid-orifice combination in all cases. The average C_d value was 0.64 in the turbulent region. Each model liquid in the laminar regime resulted in a unique relationship. Using an idea of an effective shear rate for flow through the orifice, a new Reynolds number has been defined for the different liquids to consolidate the C_d-Re relationship to the Newtonian liquid curve. A single composite model was used to predict the relationship between C_d and Re for all liquids-orifices combinations used in this work. This can be used in the engineering designs and processes.

1. Introduction

Non-Newtonian liquids have complex and very different flow characteristics than that of simple Newtonian liquids like water and oil. These characteristics depend on the size and distribution of particles, concentration of the particles, size of the conduit, level of turbulence, temperature and dynamic viscosity of the liquids (Abulnaga, 2002). Most industrial processes consist of the elementary stage like storage and transportation of such liquids from one point to another. Very little work has been carried out on the measurement of the discharge of non-Newtonian liquids out of tanks. Dziubinski and Marcinkowski (2006) studied the flow from a tank using aqueous Carboxymethyl Cellulose solution (Power-Law fluid) through circular orifices. They analysed Newtonian liquids separately from non-Newtonian liquids; however, they did not use any yield stress liquids in their study. It is therefore desirable to check if the accuracy of measuring the flow rate of Newtonian and non-Newtonian liquids out of tanks through orifices for different liquids and orifices can be better understood.

2. Literature

A Newtonian liquid is characterised by a constant shear viscosity in laminar flow and under incompressible conditions (Myles, 2003; Chhabra and Richardson, 2008; Sochi, 2009). Non-Newtonian liquids do not have a constant viscosity, or they need a minimal external stress before they begin to shear like a viscous liquid (Malkin and Isayev, 2006; Chhabra and Richardson, 2008; Sochi, 2009). Such liquids are classified into three categories and one of the groups is time-independent liquids. If the viscosity of a liquid decreases with the increasing shear rate, the liquid is defined as pseudoplastic and if

* *Corresponding author.*
E-mail address: thamaemc@cput.ac.za (M. Khahledi).
https://doi.org/10.1016/j.cherd.2020.02.015

Nomenclature

Symbol

A_0	Area of the orifice (m^2)
a_1,b_2,	Constants in Eq. (14)
a_2,b_1	Constants in Eq. (15)
Bn	Bingham number
c,d,t	Constants in Eq. (13a,b)
C_d	Coefficient of discharge
C_{dpre}	Predicted coefficient of discharge
D	Pipe diameter (m)
d	Orifice diameter (m)
dh	Orifice hydraulic diameter (m)
F	Constant in Eqs. (12) and (16)
g	Acceleration due to gravity (m/s^2)
f_1	Slope in the laminar flow
f_2	Slope in the turbulent flow
h	Fluid height above the orifice (m)
k	Fluid consistency index (Pa s)
L	Orifice thickness (m)
n	Flow behaviour index
Q	Flow rate at the orifice (m^3/s)
Qpre	Predicted flow rate (m^3/s)
Re	Reynolds number
Re_{Gen}	Generalised Reynolds number (Eq. 6)
Re_{MR}	Metzner and Reed Reynolds number
Re_{New}	New Reynolds number (Eq. 25)
Re_2	Slatter and Lazarus Reynolds number (Eq. 8)
v	Velocity (m/s)
ρ	Fluid density (kg/m^3)
τ	Shear stress (Pa)
τ_w	Wall shear stress (Pa)
τ_y	Yield stress (Pa)
τ_y^B	Bingham yield stress (Pa)
μ	Viscosity (Pa s)
μB	Bingham viscosity (Pa s)
μeff	Effective viscosity (Pa s)
$\dot{\gamma}$	Shear rate (l/s)
$\dot{\gamma}_{eff}$	Effective shear rate (1/s)
α	Constant in Eq. (28)

the liquid needs a threshold stress before flowing it is called a yield stress liquid.

The Herschel–Bulkley model can be used for characterising the non-Newtonian liquids for this class of non-Newtonian liquid behaviour (Chhabra and Richardson, 2008). It is written as

$$\tau = \tau_y + k\dot{\gamma}^n \quad (1)$$

In the limit of n = 1, Eq. (1) reduces to the familiar Bingham plastic model as

$$\tau = \tau_y + k\dot{\gamma}^n \quad (2)$$

Similarly, in limit of τ_y = 0, Eq. (1) reduces to the familiar Power-Law model as:

$$\tau = k\dot{\gamma}^n \quad (3)$$

Thus, depending upon the choice of a non-Newtonian viscosity model, different dimensionless parameters emerge for a given application. In the present case of the discharge through an orifice, the Bingham number as shown in Eq. (4), expresses the viscoplastic characteristics of a non-Newtonian liquid (Thompson and Soares, 2016).

$$Bn = \frac{\tau_y^B D}{\mu_B v} \quad (4)$$

Discharge coefficient (C_d) is expected to be a function of Oldroyd C_d number (Od), Reynolds number (Re), Power-Law index (n) for a given orifice, i.e.

$$C_d = f(Od, Re, n) \quad (5)$$

The Reynolds number (Re) is a ratio of the inertial forces to viscous forces. The generalised Reynolds number is given which can be applied for any rheological viscosity model (only influences the value of τ_w).

$$Re_{Gen} = \frac{8\rho v^2}{\tau_w} \quad (6)$$

Thus, for instance the pipe Reynolds number for Newtonian liquids is expressed as:

$$Re = \frac{\rho v D}{\mu} \quad (7)$$

For non-Newtonian liquids, there are different Reynolds number definitions available in the literature, that have been derived from the generalised Reynolds number and for Herschel–Bulkley liquids it is defined as follows (Slatter and Lazarus, 1993):

$$Re_2 = \frac{8\rho v^2}{\tau_y + k\left(\frac{8v}{D}\right)^n} \quad (8)$$

In orifice flow it has been shown that the coefficient of the discharge (C_d) value is a strong function of the Reynolds number, especially in the laminar flow regime (Joye and Barrett, 2003). An orifice C_d is a function of the orifice geometry, liquids properties and flow characteristics. For turbulent flow 0.62 is commonly used value for sharp crested orifices. But Spencer (2013), suggested the discharge coefficient to vary in the range 0.60–0.64, in-line with the findings of Boss (1989) depending on the orifice diameter. Prohask (2008), conducted experiments that show the effect of orifice diameter on the discharge coefficient. They concluded that the smaller the orifice diameter, the higher the coefficient of discharge, and as the size of the orifice increases, the coefficient of discharge decreases.

Orifice flow rate relation typically starts with the application of the Bernoulli equation (Prohask, 2008) and the theoretical velocity at the outlet is given as:

$$v = \sqrt{2gh} \quad (9)$$

where h is the height of the liquid above the orifice. Eq. (9) represent the maximum theoretical discharge through the orifice. Due to the end effects and non-uniformity effects, the actual velocity is given as:

$$V_{actual} = C_d\sqrt{2gh} \quad (10)$$

where C_d accounts for deviation from ideal condition,

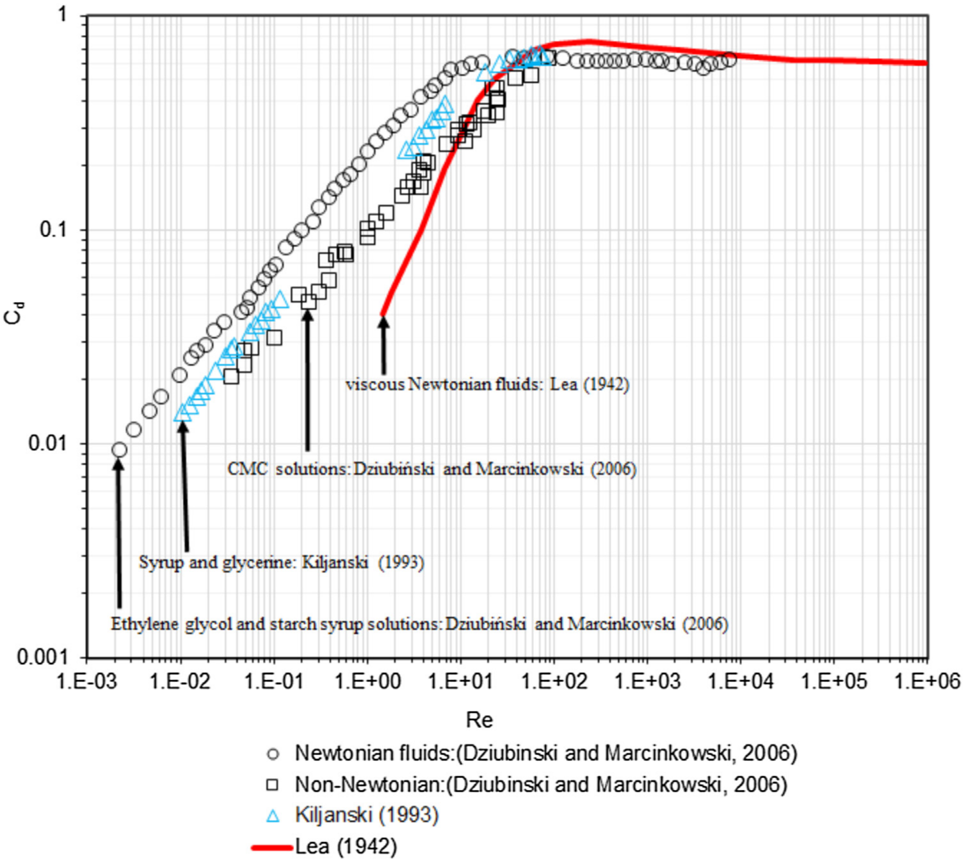

Fig. 1 – C_d-Re relationship for Newtonian and non-Newtonian liquids (Dziubinski and Marcinkowski (2006); Kiljanski, 1993 and Lea, 1942).

and

$$Q_1 = C_d A_0 \sqrt{2gh} \tag{11}$$

Swamee and Swamee (2010); Dziubinski and Marcinkowski (2006); Della Valle et al. (2000) and Kiljanski (1993) have all studied the flow rate measurement of highly viscous Newtonian liquids through circular sharp crested orifices from tanks. Sharp crested orifices can have different aspect ratios which is the length to diameter ratios (L/d) of the orifice. Marcinkowski and Dziubinski (2004) and Dziubinski and Marcinkowski (2006) studied the flow of non-Newtonian Power-Law liquids from different diameter orifices. They used orifices with aspect ratios 0, 0.35, 0.5, 0.75, 1 and 3 and diameters 5, 8,12.5 and 17 mm. They tested different concentrations of CMC solutions and the average C_d value was found to be 0.67 in the turbulent region, which is slightly higher than the oft-quoted value of 0.62 in the context of Newtonian liquids. They established a relationship between C_d values and Re_{MR}, but argued that the shear rate obtained from the discharge of orifices from tanks is not given by 8v/d as it is for pipe flows. Therefore, the shear rate for an orifice is postulated to be given by

$$\dot{\gamma} = \frac{Fv}{d} \tag{12}$$

where F is a proportionality constant to reduce the non-Newtonian Re to Newtonian conditions.

Limited experimental results for suspensions and polymer solutions indicate that $F \leq 8$, which is in agreement with the study conducted by Della Valle et al. (2000), where suspensions of delaminated kaolin clay mixed with polyethylene glycol and water (non-Newtonian liquids) were tested. A round orifice was fitted between two identical cylindrical tanks and the measured pressure drop was used to calculate Re and the Euler number (Eu). The value of the factor F was not given in the studies of Dziubinski and Marcinkowski (2006) and Della Valle et al. (2000). Kiljanski (1993) studied the discharge of highly viscous Newtonian liquids through orifices with aspect ratios of 0, 0.5 and 1 from the bottom of a tank. They measured the discharge rate under a constant head for a given time. Brater et al. (1996) re-analysed the Lea (1942) results where they measured the discharge of highly viscous Newtonian liquids from a tank using orifices. The Dziubinski and Marcinkowski (2006); Kiljanski (1993) and Lea (1942) results for L/d of 0 are shown in Fig. 1. The Newtonian liquids' C_d values from the Dziubinski and Marcinkowski (2006) results are at lower Reynolds numbers as compared to the Kiljanski (1993) values. This might be because of the size of orifice used and difference in experimental set-up.

The flow rate measurement of water through sharp crested circular and square orifices with the same hydraulic diameters was conducted by Smith (1886) and presented by Brater et al. (1996). The geometry of the orifices did not seem to affect the flow and the C_d values of the orifices. Some studies through different shapes of orifices have been reported for flow in pipes, and for Newtonian liquids. Circular and square orifices with the same flow area had the same C_d values, but the triangular orifice had a much higher C_d value (Novak and Koza, 2013). Research by Elsaey et al. (2014); van Melick and Geurts (2013) and El-Azm et al. (2010) analysed the pressure drop versus Re for flow through circular, square and triangular orifices. In laminar flow the pressure drop was higher for square and triangular orifices, but in turbulent flow the circular orifice had higher pressure drops (Elsaey et al., 2014;

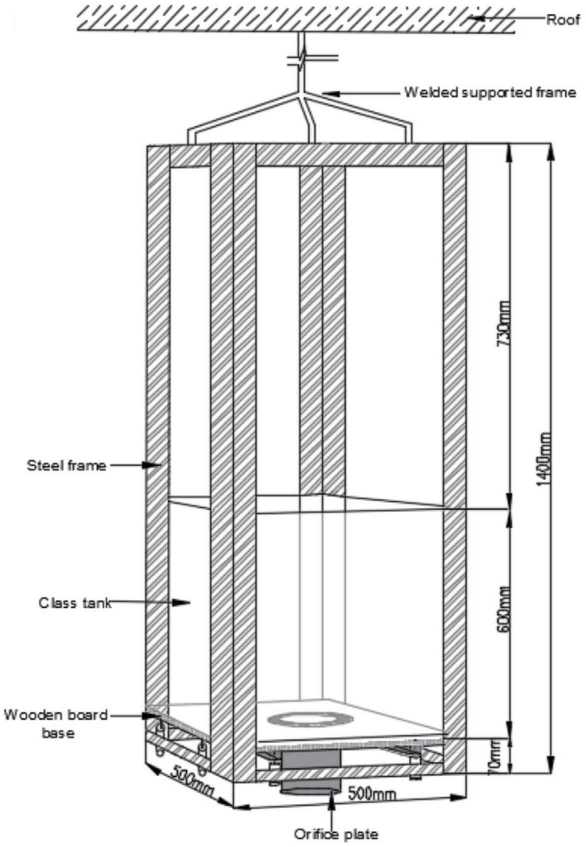

Fig. 2 – A rectangular tank supported by steel frame.

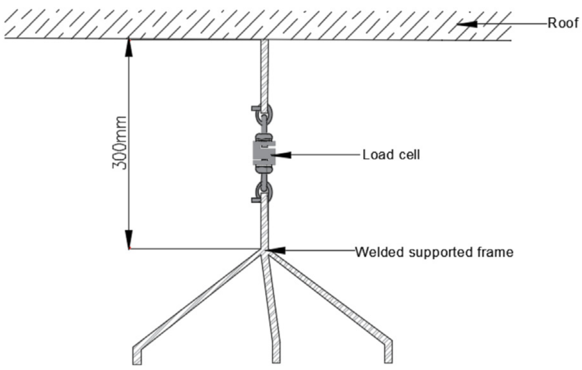

Fig. 3 – load cell.

van Melick and Geurts, 2013). El-Azm et al. (2010) however established the same pressure drop for triangular and circular orifices. These studies through different shapes of orifices were all done in pipes, and for Newtonian fluids.

3. Method

The test rig used in this work consists of a square tank (400 × 400 × 600 mm and weighing 42.1 kg) fitted with an orifice plate at the bottom (Fig. 2). A load cell attached to the tank by steel frames was used to measure the discharge rate (Fig. 3). Four different sizes of sharp crested square, triangular and circular orifices with 8 mm, 12 mm, 16 mm and 20 mm hydraulic diameters and L/d ratio of 0 were used as shown in Fig. 4. The orifices were made of polyvinyl chloride (PVC). The tests were done in batch mode where the tank was filled and emptied through the orifices. The change in voltage with time for the load cell was recorded during the discharge of the liquids. The voltage was converted to weight from which the liquid height could be calculated as a function of time and a height versus time graph was produced. A second order polynomial was fitted to the data and its slope gave the value of dh/dt, i.e. velocity as a function of liquid height above the orifice. Its derivative was used to compute the discharge at any time. The C_d values were calculated using Eq. (10).

The shear rate calculated from the flow rate measurement through the orifices ranged between ±200 s^{-1} and ±2600 s^{-1}. The shear rate range used for rheological tests varied from 100 s^{-1} to 1000 s^{-1}, to correspond with the application shear rate obtained from flow through the orifices. The measurements for the shear rates that were less than 100 s^{-1} were unstable and the shear rates greater than 1000 s^{-1} were in the turbulent region for the cup and bob geometry used in the rheometer.

Rheological characterisation (shear stress, shear rate and normal stresses) of the test liquids were carried out at the same temperature as that which was encountered in the flow test rig. A Paar Physica MCR 300 rheometer was used to determine the rheological properties of the liquids. The measuring bob and a cup with diameters 13.33 mm and 14.46 mm respectively were used to conduct the test. The measuring gap was 1.13 mm. The liquids' physical and rheological properties are reported in Table 1.

Water was used as the Newtonian liquid to calibrate the orifices. Different concentrations of glycerine, Carboxmethyl Cellullose (CMC) solutions and kaolin and bentonite suspensions were prepared and used as test liquids in this study. Glycerine was mixed with water to form a glycerine solution and immediately tested to avoid water absorption. CMC, kaolin and bentonite are in powder form and their required amounts were mixed with water to form liquid suspensions. The kaolin suspension was given three days to hydrate. Bentonite suspensions and CMC solutions were allowed to homogenously mix for five days. An electric mixer was attached to the mixing tank to stir the liquids continuously. The liquids were mixed before being transferred to the tank. Each liquid was allowed to flow through the tank at least twice before the data was collected. The liquid temperature was recorded before and after the flow rate tests. Samples of the test liquids were stored in a water-tight container before and after the flow rate test, in order to carry out the relative density and rheology tests.

Eqs. (7) and (8) were used to calculate the respective Reynolds numbers. The hydraulic diameter was used in the definition of the Re. The relationship between C_d values and Reynolds numbers was determined.

A composite curve fitting procedure was used to predict the model that is used to express the discharge of Newtonian and non-Newtonian liquids through orifices from a tank. The composite curve fitting has been used in the literature amongst others by Garcia et al. (2003); Haldenwang et al. (2012); Khahledi et al. (2014) to predict the range of f-Re and C_d-Re relationship for different multiphase liquids in pipes and flow through weirs. This method is described in detail by Patankar et al. (2002). The curve is fitted by a composite power-law correlation as shown in Eq. (13a).

$$C_d = f_2 + \frac{(f_1 - f_2)}{\left(1+\left(\frac{Re}{t}\right)^c\right)^d} \tag{13a}$$

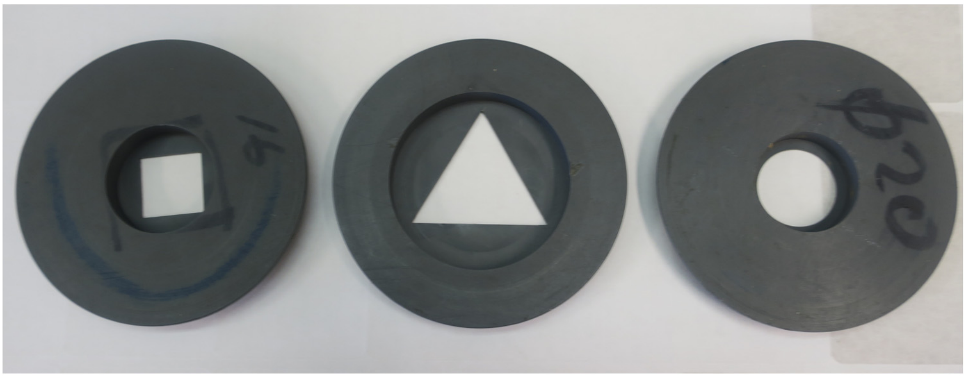

Fig. 4 – Square, triangular and circular orifices geometry.

Table 1 – Rheological parameters of the test liquids.

Fluid	Conc. %	Density kg/m^3	k Pa s^n	n	τ_y Pa	μ Pa s	$\dot{\gamma}$ from the orifice s^{-1}	Temp. °C
Kaolin v/v	20.3	1336	3.98	0.36	39.4	–	541–2318	16
	13.1	1217	0.067	0.72	8.9	–	821–2294	18
CMC w/w	7.55	1043	2.39	0.64	–	–	416–2276	18
	6.58	1037	0.882	0.70	–	–	527–2382	18
	5.21	1029	0.206	0.79	–	–	563–2518	18
	2.81	1016	0.017	0.97	–	–	508–2487	18
	2.40	1014	0.006	1.00	–	–	605–2606	25
Bentonite w/w	7.3	1046	0.021	1.00	30.5	–		21
	6.99	1044	0.014	1.00	15.7	–	653–2606	17
	3.77	1023	0.006	1.00	1.13	–	574–2571	18
Glycerine v/v	100	1258	–	–	–	0.973	212–1870	18
	96	1248	–	–	–	0.304	467–1786	19
	93	1242	–	–	–	0.129	435–1756	17
	65	1179	–	–	–	0.019	515–2406	18

where f_1 (Eq. 14) is fitted in the laminar region to obtain a_1 and b_1.

$$f_1 = a_1 Re^{b_1} \tag{14}$$

Similarly, f_2 (Eq. 15) is fitted in the turbulent region to determine a_2 and b_2.

$$f_2 = a_2 Re^{b_2} \tag{15}$$

Eq. (13a) is then fitted to all the data points to determine parameters c, d and t. The non-linear optimisation method of Microsoft excel solver minimising the residual mean square of the predicted values is used to obtain the parameters of the composite equation.

4. Results and discussion

Calibration results for circular, square and triangular orifices are shown in Fig. 5. The average C_d values for these orifices is 0.62 which agrees with the average C_d values reported by Dziubinski and Marcinkowski (2006) for flow through sharp crested circular orifices from tanks. The C_d values obtained for these orifices are within ±4% compared to the average C_d value of 0.62. It can therefore be concluded that the various shapes of the orifices with the same hydraulic diameter do not affect the flow rate in the turbulent region.

The Reynolds number and C_d values for circular, square and triangular orifices for all the liquids are plotted in Fig. 6. The C_d values for non-Newtonian liquids in the turbulent region coincide with the Newtonian C_d values. Therefore, the average C_d values for all the orifices and liquids in the turbulent region is approximately 0.64 which is at slight variance with the value of 0.67 reported by Dziubinski and Marcinkowski (2006) for non-Newtonian liquids. However, their results correspond to orifices with different L/d ratios. In the laminar flow region, the Re-values for Newtonian liquids start at lower values than the non-Newtonian liquids' Re-values and the Dziubinski and Marcinkowski (2006) results show a similar trend. Non-Newtonian liquids have different flow behaviour than Newtonian liquids because of their different liquid properties. Each liquid model (Power-Law, Herschel–Bulkley and Bingham) exhibits a different flow behaviour in the laminar region. The Re values for glycerine start from Re = 10, CMC solution from Re = 70, kaolin suspension from Re = 200 and bentonite suspension from Re = 400. This shows the effect of yield stress and viscosity of the non-Newtonian liquids.

Fig. 7 shows a comparison between the current study and that of others including Dziubinski and Marcinkowski (2006); Kiljanski (1993) and Lea (1942). Each study is seen to have its own curve, thus each orifice should be calibrated and analysed as per calibration results which makes it cumbersome for engineering design purposes. Fester et al. (2008) demonstrated, albeit for pressure loss coefficients in sudden pipe contractions, that this difficulty can be overcome by adequately accounting for the viscous properties of the liquids in the Reynolds number. However, Fig. 7 clearly shows that the use of the generalised Reynolds number utilising 8v/D as the effective shear rate, fails to do the same in the case of the discharge coefficient for gravitational flows from tanks in laminar flow. A new Reynolds number to account for the effec-

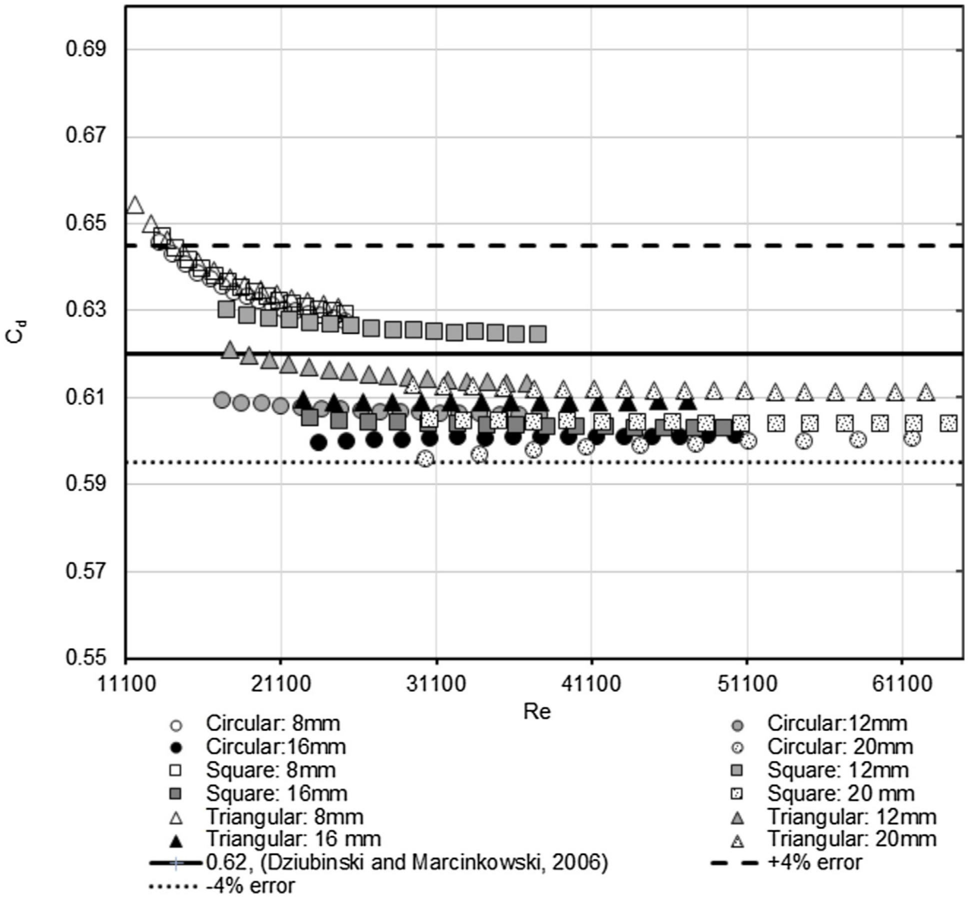

Fig. 5 – Calibration results for circular, square and triangular orifices.

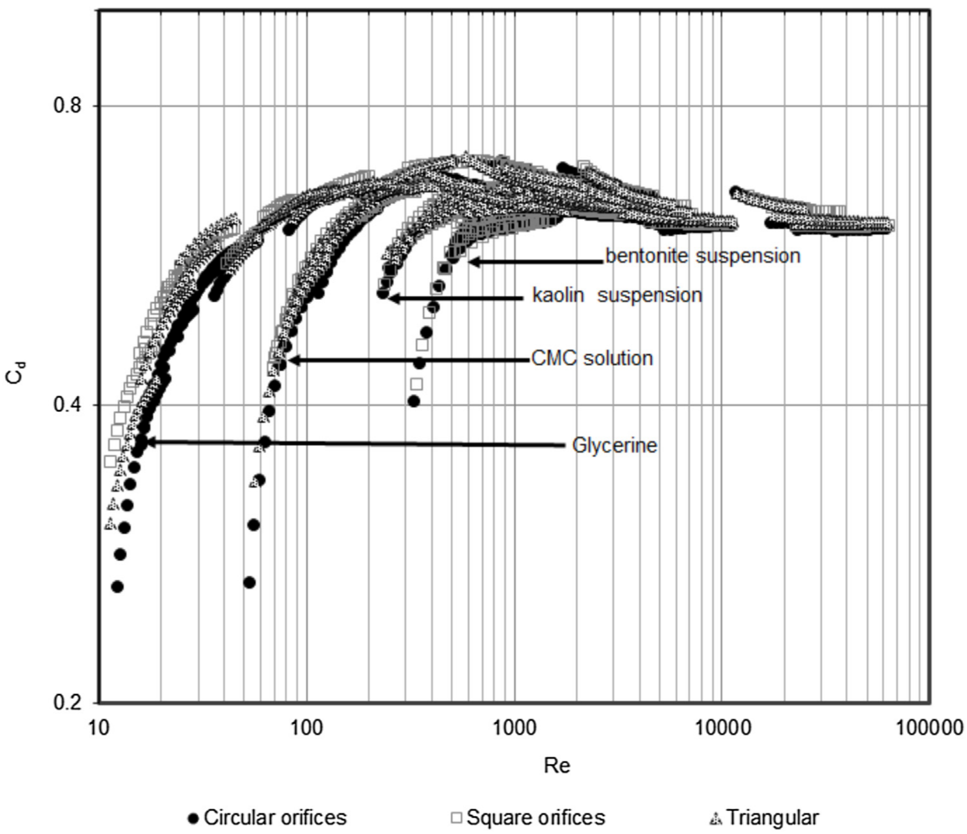

Fig. 6 – C_d-Re relationship for Newtonian and non-Newtonian liquids for circular, square and triangular orifices.

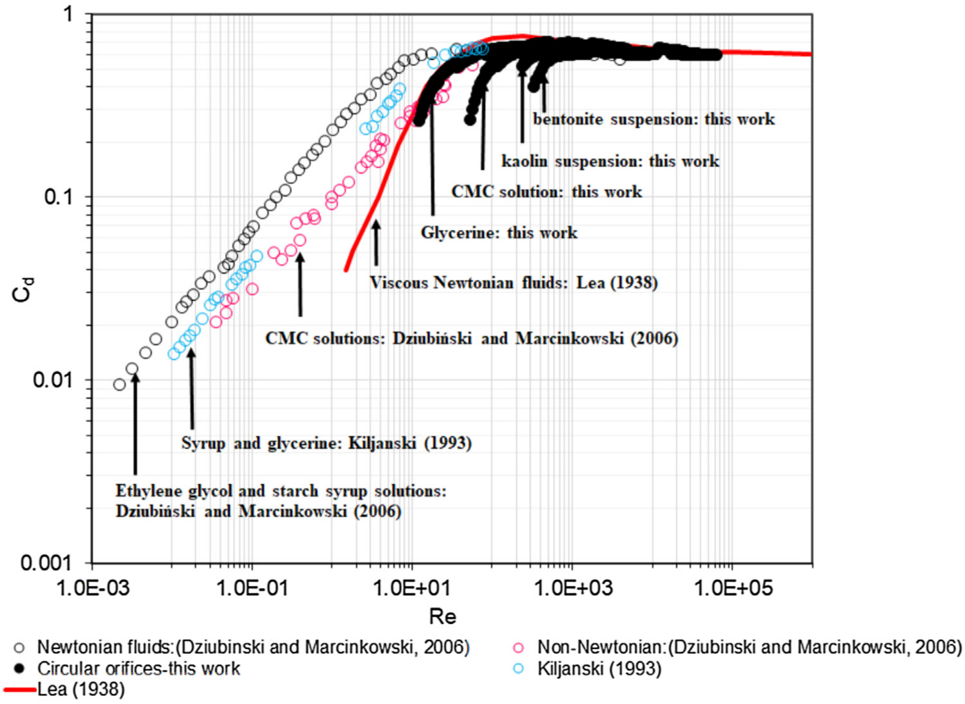

Fig. 7 – C_d vs Re for Newtonian and non-Newtonian liquids for L/d of 0 (this work, Dziubinski and Marcinkowski, 2006; Kiljanski, 1993; Lea, 1942).

tive shear rate as postulated by Marcinkowski and Dziubinski (2004) and the incorporation of the yield stress is given below.

5. Model prediction

Marcinkowski and Dziubinski (2004) and Della Valle et al. (2000) indicated that the average shear rate calculated from the discharge of orifices from tanks is not given by 8v/d, though it is expected to be proportional to v/d. Hence one can postulate that the average shear rate $\dot{\gamma}$ is given by:

$$\dot{\gamma}_{eff.} = \frac{Fv}{d} \tag{16}$$

where F is constant which is smaller than 8, the value for flow in a tube.

Therefore, the effective viscosity of the liquid would be given as:

$$\mu_{eff} = \frac{\tau}{\dot{\gamma}_{eff}} \tag{17}$$

Substituting the effective shear rate in Herschel–Bulkley liquid model the shear stress is given as:

$$\tau = \tau_y + k\dot{\gamma}_{eff}^{n} \tag{18}$$

Combining Eqs. (17) and (18)

$$\mu_{eff} = \frac{\tau_y + k\dot{\gamma}_{eff}^{n}}{\dot{\gamma}_{eff}} \tag{19}$$

Thus

$$\mu_{eff} = \frac{\tau_y + k\left[\frac{Fv}{d}\right]^n}{\frac{Fv}{d}} \tag{20}$$

or

$$\mu_{eff} = k\left(\frac{Fv}{d}\right)^{n-1}\left[\frac{\tau_y}{k\left(\frac{Fv}{d}\right)^n} + 1\right] \tag{21}$$

But the Bingham number is given as:

$$Bn = \frac{\tau_y^B D}{\mu_B v} = \frac{\tau_y}{k\left(\frac{Fv}{d}\right)^n} \tag{22}$$

Therefore

$$\mu_{eff} = k\left(\frac{Fv}{d}\right)^{n-1}[1+Bn] \tag{23}$$

The substitution of effective viscosity in the definition of Re is given as:

$$Re = \frac{\rho v d}{\mu} = \frac{\rho v d}{\mu_{eff}} = \frac{\rho v d}{k\left(\frac{Fv}{d}\right)^{n-1}(1+Bn)} = \frac{\rho v^{2-n} d^n}{kF^{n-1}(1+Bn)} \tag{24}$$

Therefore, the interim Re is:

$$Re_{(new)} = \frac{\rho v^{2-n} d^n}{kF^{n-1}(1+Bn)} \tag{25}$$

For the Bingham Model: n = 1
For the Power law model: Bn = 0
And for Newtonian fluids: n = 1

In order to determine the value of F, composite curve fitting (Eq. (13b)) as described by Patankar et al. (2002) was used to predict the fit for Newtonian liquids.

$$C_d = f_2 + \frac{(f_1 - f_2)}{\left(1+\left(\frac{Re}{t}\right)^c\right)^d} \tag{13b}$$

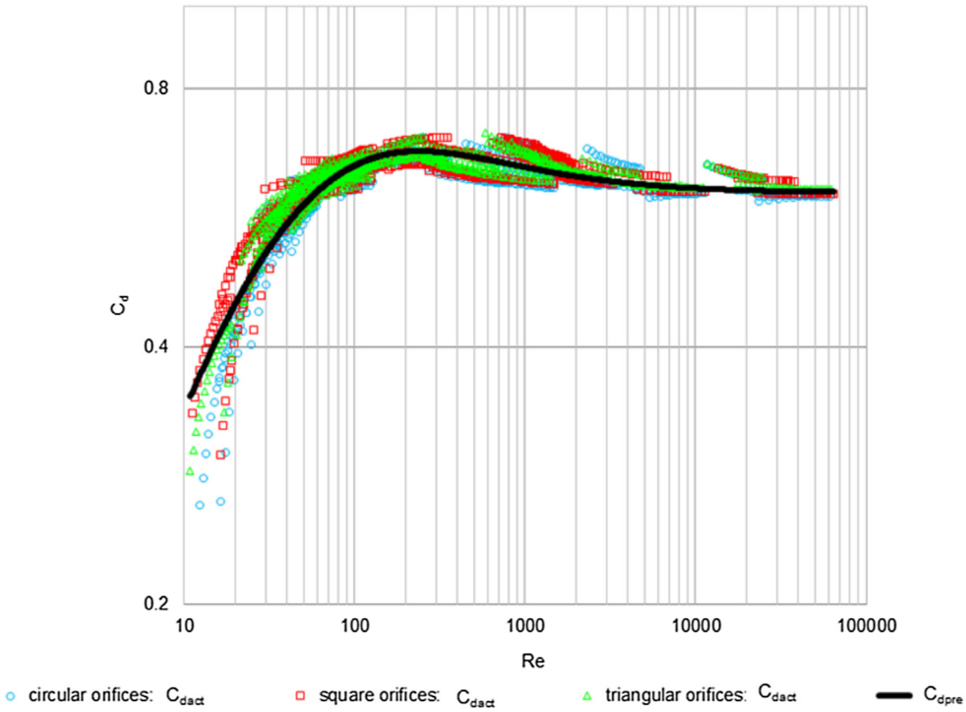

Fig. 8 – $C_{d(actual)}$ and $C_{d(pred)}$ versus Reynolds numbers.

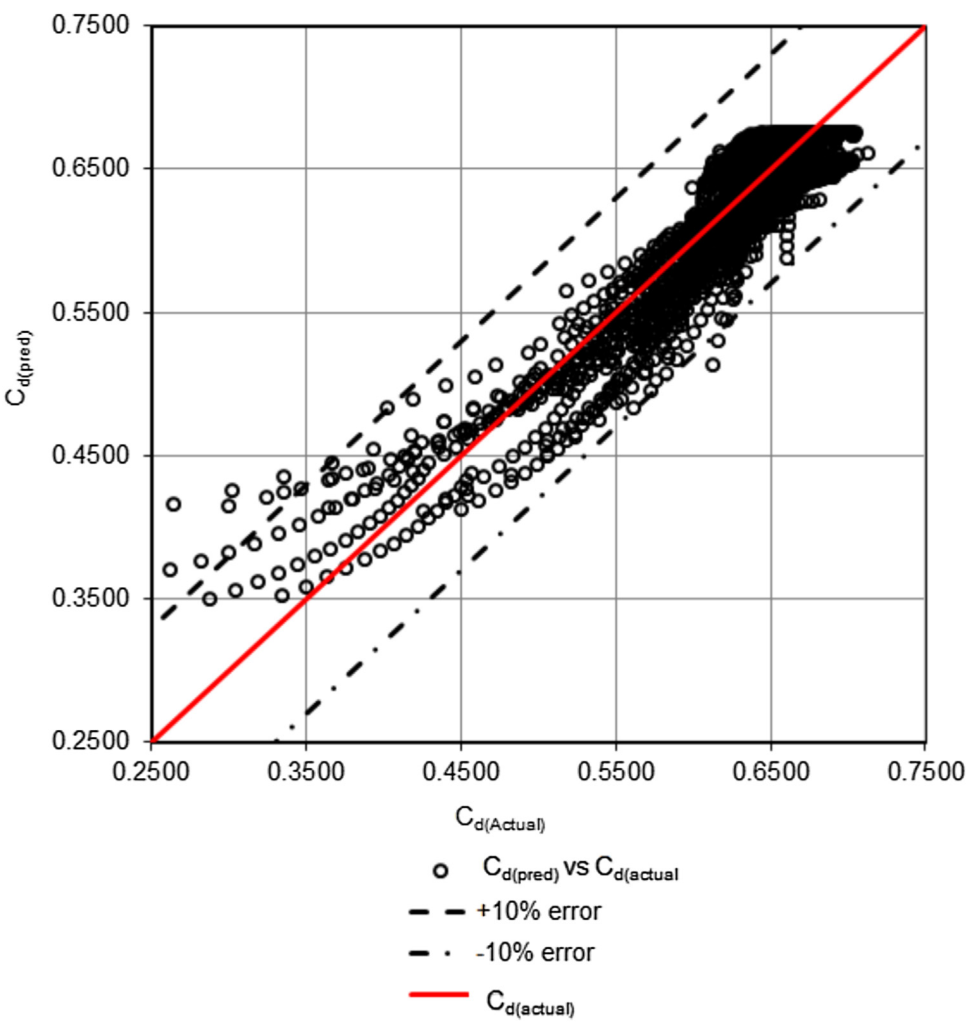

Fig. 9 – $C_{d(pred)}$ versus $C_{d(actual)}$.

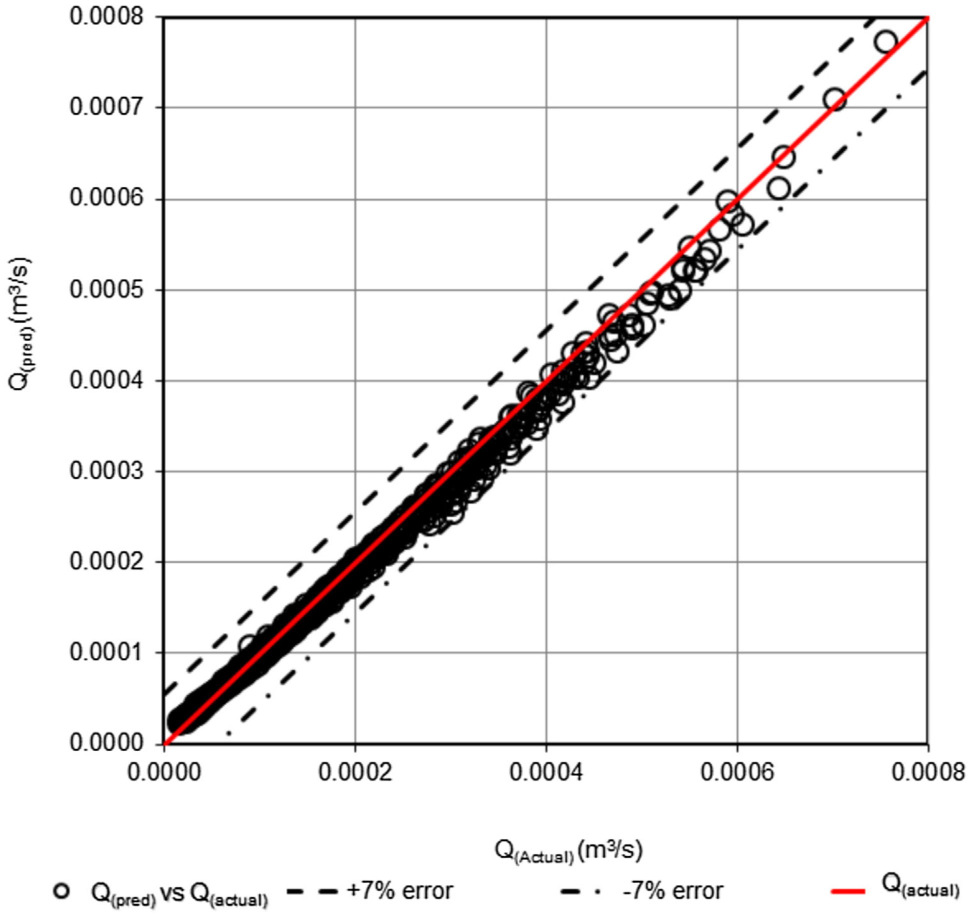

Fig. 10 – $Q_{(pred)}$ versus $Q_{(actual)}$ for laminar flow.

This fitting was applied to all the orifice shape results. f_1 for circular, square and triangular orifices was found to be $0.083Re^{\circ.49}$ and f_2 was 0.62. Eq. (13b) was optimised and the values obtained for t, c and d were 50, 1.26 and 1.43 respectively.

Therefore, the predicted C_d value for Newtonian liquids for circular, square and triangular orifices is as shown in Eq. (26).

$$C_d = 0.62 + \frac{\left(0.083Re^{0.49} - 0.62\right)}{\left(1 + \left(\frac{Re}{50}\right)^{1.26}\right)^{1.43}} \quad (26)$$

The new Reynolds number (Re_{new}) Eq. (27) was calculated for Power law liquids in the laminar flow for each orifice shape.

$$Re_{(new\text{-}PL)} = \frac{\rho v^{2\text{-}n} dh^n}{kF^{n\text{-}1}} \quad (27)$$

The Newtonian predicted C_d in Eq. (26), was used to calculate the predicted C_d values for CMC solutions using the new Reynolds number (Eq. (27)). The values of F were determined by the optimisation for CMC solution in the laminar region for each orifice shape. The average F value for circular, square and triangular orifices and for all power-law liquids, was found to be 0.3.

The Re_{new} values for all the liquids were calculated using the F value of 0.3. The Herschel–Bulkley liquids were adjusted by the factor (α) to adjust the Re to Newtonian liquids as illustrated in Eq. (28).

$$Re_{(new\text{-}HB)} = \frac{\rho v^{2\text{-}n} dh^n}{kF^{n\text{-}1}(1 + \alpha Bn)} \quad (28)$$

A Newtonian composite curve fitting was applied to kaolin suspensions and the value of α was determined by the optimisation for all the orifice shapes. The average factor (α) of 0.2 was obtained for circular, square and triangular orifices.

The new Reynolds numbers were calculated for all non-Newtonian liquids using the following established Re_{new} equations:

For the Herschel–Bulkley model:

$$Re_{(new\text{-}HB)} = \frac{\rho v^{2\text{-}n} dh^n}{k0.3^{n\text{-}1}(1 + 0.2Bn)} \quad (29)$$

For the Bingham model:

$$Re_{(new\text{-}BP)} = \frac{\rho v dh}{k(1 + Bn)} \quad (30)$$

where Bn is:

$$Bn = \frac{\tau_y}{k\left(\frac{0.3v}{dh}\right)^n} \quad (31)$$

For the Power-Law model:

$$Re_{(new\text{-}PL)} = \frac{\rho v^{2\text{-}n} dh^n}{k0.3^{n\text{-}1}} \quad (32)$$

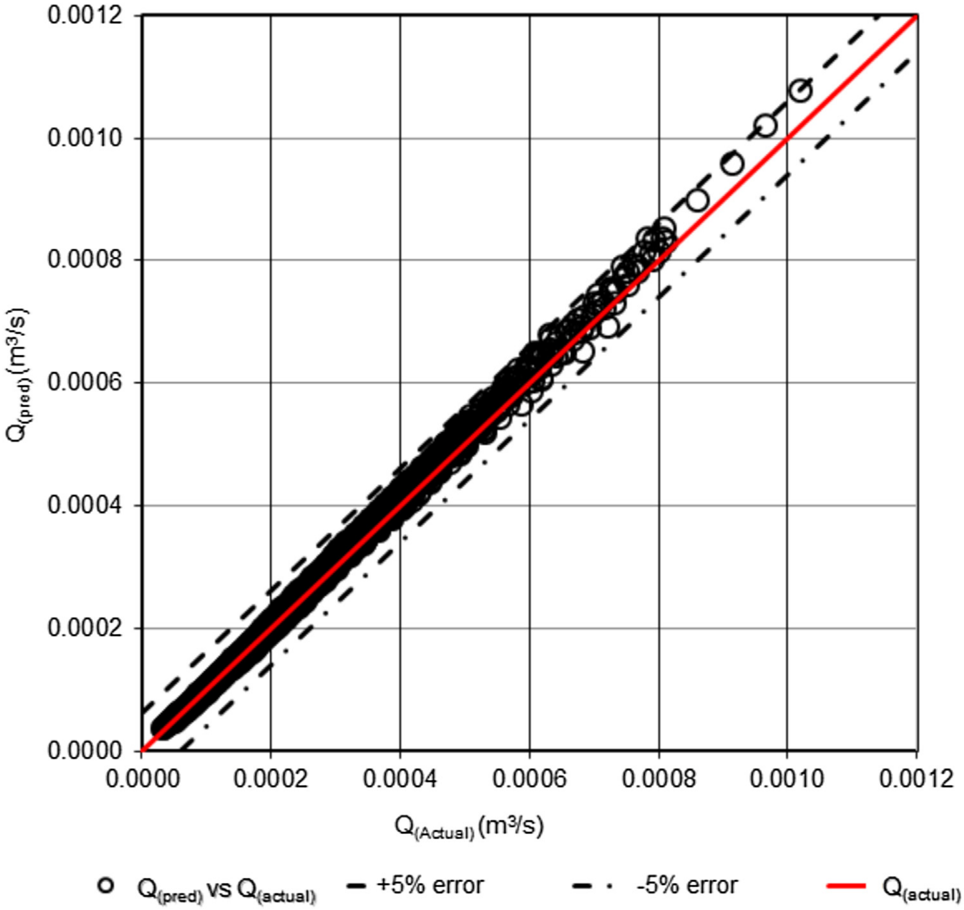

Fig. 11 – $Q_{(predl)}$ versus $Q_{(actual)}$ for transition flow.

The new fitting curve was established by applying a single composite equation to all the orifices data using the new Reynolds number values for non-Newtonian liquids. The values of f_1 and f_2 became $0.057Re^{\circ.58}$ and 0.61 respectively. After the non-linear optimisation method minimising the residual mean square of the single composite equation, the actual C_d and predicted C_d values versus Reynolds number curve was plotted (Fig. 8) and the combined C_d equation for circular, square and triangular orifices was established (Eq. 33). 98% of the actual C_d values are within a $\pm 10\%$ range when compared to the predicted C_d values (Fig. 9). Eq. (33) is applicable for the following range of conditions: 8 mm < d < 20 mm, 0 < L/d < 0.125 and 10 < Re < 65000.

$$C_{d(pred)}=0.61+\frac{\left(0.057Re^{0.58}\text{-}0.61\right)}{\left(1+\left(\frac{Re}{80}\right)^{0.758}\right)^{1.98}} \tag{33}$$

The predicted flow rate is expressed in Eq. (34). The error margins between the actual and predicted discharge for laminar, transition and turbulent flows are at $\pm 7\%$, $\pm 5\%$ and $\pm 2\%$ respectively as shown in Figs. 10–12.

$$Q_1 = C_{d(pred)} A_0 \sqrt{2gh} \tag{34}$$

This equation is applicable to orifices with an L/d of 0 fitted at the bottom of the tank and for a Reynolds number range from 10 to 100 000.

6. Conclusions

The calibration results for all the orifices indicated that different shapes of orifices with equal hydraulic diameters do not have an effect in the discharge. Highly viscous Newtonian liquids and non-Newtonian liquids were tested. The rheological parameters of the liquids were determined and used to determine the Reynolds number. The C_d-Re relationship was established for all the liquids. It was found that each liquid model had its own flow trend with Newtonian liquids Re starting from Re = 10, power-law from Re = 70, Herschel–Bulkley from Re = 200 and Bingham from Re = 400. The new Reynolds number equations were derived acknowledging that the shear rate is not 8v/d as indicated by Marcinkowski and Dziubinski (2004) and Della Valle et al. (2000). A single composite equation was applied to the data obtained for the Newtonian liquids for each orifice shape. The equation was used to determine the constants (F and α) which were used to calculate the new Re for non-Newtonian liquids for gravitational flow through orifice plates from the bottom of a tank. A single composite equation was applied to all the data for all the liquids and orifices (C_d values and Re values for Newtonian liquids and new Re values for non-Newtonian liquids). The C_d versus Re laminar flow relationship yielded $0.068Re^{0.55}$ and the average C_d value in the turbulent flow was found to be 0.61. The predicted C_d equation was established, and a new discharge equation derived. This equation can be used in process engineering and design for flow of non-Newtonian liquids through sharp crested orifices.

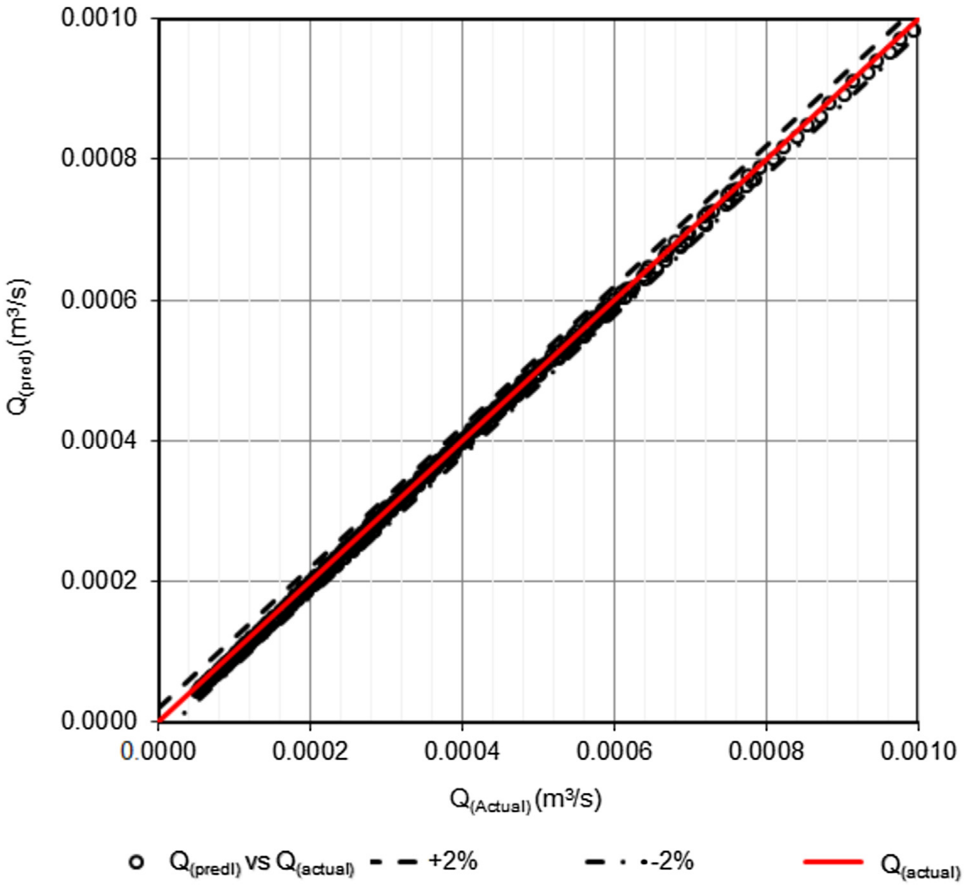

Fig. 12 – $Q_{(pred)}$ versus $Q_{(actual)}$ for turbulent flow.

Acknowledgements

The authors would like to thank the Department of Higher Education and training (Republic of South Africa) for giving Mrs. M. Khahledi an opportunity to be the nGap candidate, FPRC, CPUT for the facility, Miss Mohajane, Mr. Sutherland, Mr. du Toit, Mr. Xashimba and Mr. Mahobane for technical support, Mr. George for assistance with rheology tests and Mr. Makhaluza for administrative support.

References

Abulnaga, B.E., 2002. Slurry Systems Handbook. USA: McGraw Hill, New York.
Brater, E.F., King, H.W., Lindell, J.E., Wei, C.Y., 1996. Handbook of Hydraulics for the Solution of Hydraulic Engineering Problems, 7th ed. McGraw-Hill, New York.
Chhabra, R.P., Richardson, J.F., 2008. Non-Newtonian Flow and Applied Rheology in Engineering Applications, 2nd ed. Elsevier, Oxford (UK).
Della Valle, D., Tanguy, P.A., Carreau, P.J., 2000. Characterization of the extensional properties of complex fluids using an orifice flowmeter. J. Non-Newtonian Fluid 94, 1–13.
Dziubinski, M., Marcinkowski, A., 2006. Discharge of Newtonian and non-Newtonian liquids from tanks. Chem. Eng. Res. Des. 84 (A12), 1191–1198.
El-Azm, Abou, Aly, A., Chong, A., Nicolleau, F., Beck, S., 2010. Experimental study of the pressure drop after fractal-shaped orifices in turbulent pipe flows. Exp. Therm. Fluid Sc. 34, 104–111.
Elsaey, A., Abou El-Azm Aly, A., Fuoad, M., 2014. CFD simulation of fractal-shaped orifices for flow measurement improvement. Flow Meas. Instrum. 36, 14–23.
Fester, V., Mbiya, B., Slatter, P., 2008. Energy losses of non-Newtonian fluids in sudden pipe contractions. Chem. Eng. J. 145, 57–63.
Garcia, F., Garcia, J.C., Padrino, J.C., Mata, C., Trallero, J.C., Joseph, D.D., 2003. Power law and composite power law friction factor correlations for laminar and turbulent gas-liquid flow in horizontal pipelines. Int. J. Multiph. Flow 29, 1605–1624.
Haldenwang, R., Sutherland, A.P.N., Fester, V.G., Holm, R., Chhabra, R.P., 2012. Sludge pipe flow Pressure drop prediction using composite power-law friction Factor-Reynolds number correlation based on different non-Newtonian Reynolds numbers. Water SA. 38 (4), 615–622.
Joye, D.D., Barrett, B.C., 2003. The tank drainage problem revisited: do these equations actually work. Can. J. Chem. Eng. 81, 1052–1057.
Khahledi, M., Haldenwang, R., Chhabra, R., 2014. Flow rate measurement of non-Newtonian fluids through sharp crested notches. ASCE J. Hyd. Eng. 141 (1), 04014067.
Kiljanski, T., 1993. Discharge coefficient for free jets from orifices at low Reynolds number. Tran ASME 115, 778–781.
Lea, F.C., 1942. Hydraulics, 6th ed. Longmans, Green, New York.
Malkin, A., Isayev, A., 2006. Rheology: Concepts, Methods, & Applications. Chemtec Publishing, Toronto.
Marcinkowski, A., Dziubinski, M., 2004. Discharge coefficient for discharge of non-Newtonian liquids from vessel. Chem. Process Eng. 25 (3), 1297–1302.
Myles, K., 2003. Fluid Handling Principle and Practice, 2nd ed. K Myles & Associates, South Africa.
Novak, O., Koza, V., 2013. Measuring a discharge coefficient of an orifice for an unsteady compressible flow. Paliva 5 (1), 21–25.
Patankar, N.A., Joseph, D.D., Wang, J., Barree, R.D., Conway, M., Asadi, M., 2002. Power law correlations for sediment transport in pressure driven channel flows. Int. J. Multiphase Flows 28, 1269–1292.

Prohask, D., 2008. Investigation of the Discharge Coefficient for Circular Orifices in Riser Pipes. Clemson University pprohas@clemson.edu.

Slatter, P.T., Lazarus, J.H., 1993. Critical flow in slurry pipelines. In: Proceedings, Hydrotransport-12: 12th International Conference on Slurry Handling and Pipeline Transport, Brugge, Belgium, pp. 639–654.

Smith, H., 1886. Hydraulics: The Flow of Water through Orifices, Over Weirs, and Through Open Conduits and Pipes. Trübner and CO; John Wiley and Sons.

Sochi, T., 2009. Single-Phase Flow of Non-newtonian Fluids in Porous Media. Technical Report. Department of Physics and Astronomy, University College, London, 2009. arXiv:0907.2399v1.

Spencer, P.R., 2013. Investigation of Discharge Behaviour from a Sharp-edged Circular Orifice in Both Weir and Orifice Flow Regimes Using an Unsteady Experimental Procedure. Electronic Thesis and Dissertation Repository. Paper., pp. 1565.

Swamee, P.K., Swamee, N., 2010. Discharge equation of a circular sharp-crested orifice. J. Hydraul. Res 48 (1), 106–107.

Thompson, R.L., Soares, E.J., 2016. Viscoplastic dimensionless numbers. J. non-Newton Fluid. 238 (2016), 57–64.

van Melick, P.A.J., Geurts, B.J., 2013. Flow through a cylindrical pipe with a periodic array of fractal orifices. Fluid Dyn. Res. 45, 1–21.